WPJET3-CPR(17) 16966

B Colling et al.

# Testing of tritium breeder blanket activation foil spectrometer during JET operations

Preprint of Paper to be submitted for publication in Proceeding of 13th International Symposium on Fusion Nuclear Technology (ISFNT)

This work has been carried out within the framework of the EUROfusion Consortium and has received funding from the Euratom research and training programme 2014-2018 under grant agreement No 633053. The views and opinions expressed herein do not necessarily reflect those of the European Commission.

# Testing of tritium breeder blanket activation foil spectrometer during JET operations

Bethany Colling[a*], P. Batistoni[b], S. C. Bradnam[a], Z. Ghani[a], M. R. Gilbert[a], C. R. Nobs, L. W. Packer[a], M. Pillon[b], S. Popovichev[a] and JET Contributors**

[a]*Culham Centre for Fusion Energy, Science Centre, Abingdon, Oxon, OX14 3DB, UK*
[b]*ENEA, Department of Fusion and Technology for Nuclear Safety and Security, E. Fermi 45, 00044 Frascati (Rome), Italy*
***See the author list of "X. Litaudon et al 2017 Nucl. Fusion 57 102001"*
**Corresponding author: Bethany.Colling@ukaea.uk*

Accurate measurement of the nuclear environment within a test tritium breeding-blanket module of a fusion reactor is crucial to determine tritium production rates which are relevant to self-sufficiency of tritium fuel supply, tritium accountancy and also to the evaluation of localised power levels produced in blankets. This requires evaluation of the time-dependent spectral neutron flux within the test tritium breeding-blanket module under harsh radiation and temperature environments. The application of an activation foil-based spectrometer system to determine neutron flux density using a pneumatic transfer system in ITER has been studied, deployed and tested on the Joint European Torus (JET) machine in a recent deuterium - deuterium campaign for a selection of high purity activation foils. Deployment of the spectrometer system has provided important functional and practical testing of the detector measurement system, associated hardware and post processing techniques for the analysis of large data sets produced through the use of list mode data collection. The testing is invaluable for the optimisation of systems for future planned testing in tritium - tritium and deuterium - tritium conditions. Analysis of the time and energy spectra collected to date and the status of the development of methods for post-processing are presented in this paper.

Keywords: JET, ITER, TBM, activation, neutronics

## 1. Introduction

Activities under the EUROfusion work package (WP) JET3 programme have been established to enable the technological exploitation of the planned JET experiments over the next few years, culminating in a deuterium – tritium experimental campaign (reference DTE-2) [1]. The programme offers a unique opportunity to provide vital experimental data within the areas of nuclear technology and nuclear safety relevant to the fusion experimental facility ITER; currently under construction.

The WPJET3 subproject 'TBMD' focuses on the development and testing of detectors for the tritium breeder blankets of a fusion reactor, for example the tritium breeding test blanket modules (TBMs) that will be installed on ITER. Accurate measurement of the nuclear environment within a TBM is crucial to determine tritium production rates which are relevant to self-sufficiency of tritium fuel supply, tritium accountancy and also to the evaluation of localised power levels produced in blankets [2]. This requires evaluation of the time-dependent spectral neutron flux within the TBM under harsh radiation and temperature environments. There are few diagnostic systems that are deemed robust enough to survive those environments, though miniature fission chambers, self-powered neutron detectors, liquid scintillation techniques, diamond detectors and activation foil methods have been considered [3], [4].

During the planned D-T experimental campaign the TBMD project will take advantage of the large 14 MeV neutron fluence expected to test the use of a foil-based spectrometry detector system for evaluation of the neutron flux spectra. Practical testing of such a system and development of the post processing techniques has been performed during the recent JET deuterium – deuterium (D-D) campaign (reference C36b). This testing will be used for the optimisation of systems for future planned testing in tritium – tritium (T-T) and D-T conditions. The current status of the analyses and post processing development is presented in this paper along with a demonstration of the use of neutron spectra unfolding to determine the neutron flux.

## 2. An activation foil-based spectrometer system

A set of suitable dosimetry reactions were proposed for use in a TBM foil-based spectrometry system [5], a subset of which can be seen in table 1. Criteria such as intensity and number of emitted gamma lines and half-life were used. The proposed short half-life reactions cover a range of energy threshold and non-threshold reactions and require a limited number of different high-purity foils that will be compatible with the environmental conditions expected of the ITER TBMs. The gamma lines from the generated activation products within the foils should be readily measurable via gamma spectrometry techniques.

Under the proposed system a selection of foils, placed in a capsule, would be sent to the TBM using a pneumatic transfer system. Following irradiation the capsule would be returned via the transfer system to a shielded counting station where the neutron induced decay gamma radiation from the activated foils can be measured through spectrometry methods such as a high purity germanium (HPGe) detector.

*author's email: Bethany.Colling@ukaea.uk*

Table 1. Selected reactions from the Al, Cr and Nb foils.

| Reaction | Product half-life (s) | Approx. threshold energy (MeV) | Principle gamma line energy (keV) |
|---|---|---|---|
| $^{27}Al(n,\gamma)^{28}Al$ | 135 | - | 1779 |
| $^{27}Al(n,p)^{27}Mg$ | 568 | 4.5 | 844 |
| $^{52}Cr(n,p)^{52}V$ | 225 | 5.5 | 1434 |
| $^{53}Cr(n,p)^{53}V$ | 97 | 6 | 1006 |
| $^{54}Cr(n,p)^{54}V$ | 50 | 11 | 835 |
| $^{54}Cr(n,\alpha)^{51}Ti$ | 348 | 8.2 | 320 |
| $^{93}Nb(n,\gamma)^{94m}Nb$ | 376 | - | 871 |
| $^{93}Nb(n,\alpha)^{90m}Y$ | 11484 | 6.9 | 203 |
| $^{93}Nb(n,n'\alpha)^{89m}Y$ | 16 | 12.5 | 909 |
| $^{93}Nb(n,2n)^{92m}Nb$ | 876960 | 9.5 | 935 |

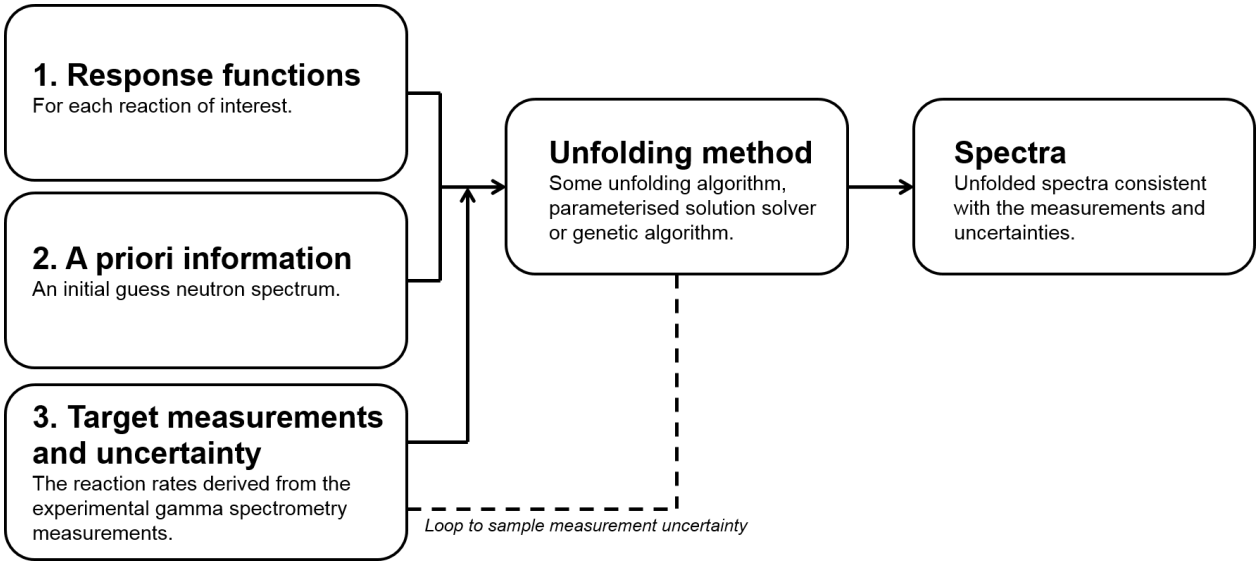


Fig. 1. General workflow for neutron spectra unfolding

The generated activity would then be determined from the characteristic spectrum. The measured activity of all reactions can then be used to unfold the neutron spectrum based on the reaction response functions, which are related to the reaction cross sections themselves.

The general workflow required to evaluate the neutron flux spectra using a foil-based spectrometry system is presented in figure 1. There are three main pieces of information required to determine a spectrum: (i) the response function of the reactions of interest, (ii) an initial guess or 'a priori' neutron spectrum, and (iii) target foil activity measurements. The unfolded spectrum, $\varnothing_{E,}$ can be described using equation 1,

$$N_k = \int R_k(E)\varnothing_E(E)\,dE \quad (1)$$

where $N_k$ is the number of counts in channel k (k = 1, n where n is the number of channels) and $R_k(E)$ is the detector response of channel k to particles of energy E.

A variety of neutron unfolding codes are available for performing the unfolding method including the UMG codes [6] of MAXED and GRAVEL, SAND-II [7] and STAYSL [8].

## 3. System testing during JET D-D operations

Experimental testing of a foil-based spectrometry system was performed during JET D-D pulses using the existing pneumatic transfer system in the JET KN2 neutron irradiation end. A number of irradiation stations are used with the KN2 system; for this test the 3-upper position (KN2 3U) was selected due to availability.

Whilst the neutron spectrum in KN2 3U differs from the spectrum that would be expected in a TBM, of benefit here is the testing of the processes and methodology, and validation of modelling which could later be generally extrapolated to more relevant TBM spectra. Part of the practical testing also aimed to assess the capability of measurement procedures with the activation foils together as a 'stack' as opposed to separating the foils and measuring each foil individually. Individual foil counting would entail a more logistically complex measurement process to be developed.

Use of the KN2 system placed restrictions on the size and mass of material that could be used due to the size

and configuration of the transfer system tubing and capsule size (figure 4). Practical testing was performed during 5 JET pulses.

### 3.2 Selection of dosimetry foils

High purity foils of Al, Cr and Nb were purchased through Goodfellow [9] at thicknesses of: Al (0.1 and 1 mm), Cr (1 and 2 mm) and Nb (1 and 2 mm). Thinner foils are proposed for testing in future D-T operations, however for testing and validation of associated processes in D-D conditions, bearing in mind the detection limits, these thicker foils were needed. Although Cs foils are proposed in [5], investigations regarding the suitability of the material for irradiation under the JET D-D environment deemed the material unsuitable.

The foils were purchased as foil sheets and the Al and Nb cut to 18 mm discs. The Cr was cut into pieces that would fit within the capsule as this was more easily achievable due to the material brittleness.

The reactions of interest from the selected Al, Cr and Nb foils are given in table 1 [5] (gamma-line data gathered from National Nuclear Data Center, Brookhaven National Laboratory [10]). A selection of different foil stack arrangements were tested. An illustrative example of a foil stack arrangement in shown in figure 2.

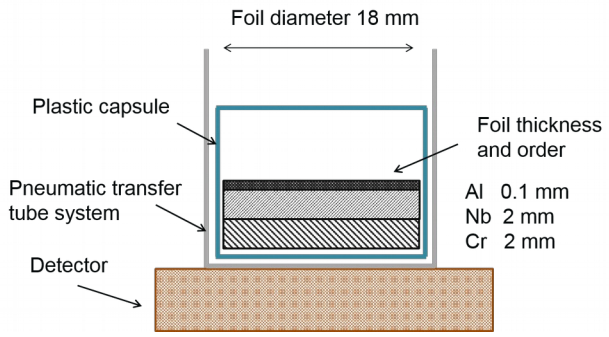


Fig. 2. Illustration of the foil arrangement and detector setup (not to scale).

### 3.3 HPGe detector and digitiser setup

Capsules containing Al, Cr and Nb were placed in the 3U irradiation station using the KN2 system during five selected JET D-D pulses, each with a unique pulse number. In this paper, analysis of data collected during one of the JET pulses (JET pulse number 92398) is presented for brevity and to illustrate the process. This was the final data set to be collected as part of this experiment.

After the capsule containing the foil stack was irradiated in the KN2 3U position, it returned to the counting station and positioned above a HPGe detector. A 20% relative efficiency JET HPGe detector was used for initial testing and subsequent measurements with a 25% relative efficiency Canberra HPGe. Both with a low background lead shield. Figure 3 shows the detector setup of the KN2 transfer system and counting station. The foils are measured within the closed lead shield to reduce background. The KN2 system capsule containing the foil stack is shown figure 4 with an example dosimetry foil.

Data acquisition processes were tested using a four-channel CAEN digitiser (DT5724) hardware [11] with list mode data acquisition and storage, where list mode acquisition allows the user to store the time stamp and pulse height of every detector event. Digitiser hardware settings were optimised for high resolution gamma spectroscopy applications; key parameter settings include a trapezoidal rise time and trapezoidal flat top time of 0.5 µs, with a preamplifier decay time matched at 40 µs. The use of list mode requires relatively large data storage, however this allows for further interrogation of the data via post processing methods. The data can be analysed over optimised acquisition time periods for each reaction, thus potentially providing a benefit in measurability of some reactions when compared with traditional methods.

Due to the use of list mode data collection, a large quantity of gamma spectra data was obtained. To interrogate the list mode data output an analysis toolkit has been developed using Python.

Fig. 3. KN2 transfer system at the counting station . Capsule inside the tube entering the lid of the low background lead shield to the detector within.

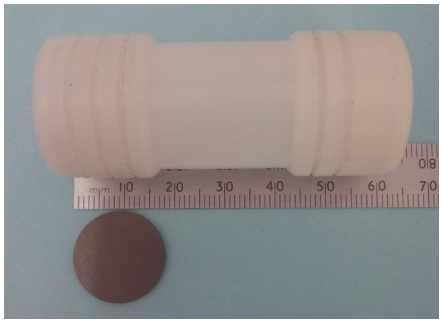

Fig. 4. Example KN2 system capsule and dosimetry foil.

To determine the activity and therefore calculate reaction rates from the measured photopeaks, the efficiency of the measurement setup is required. The detector efficiency was determined through a measurement spectrum using a standard mixed nuclide calibration source. This measured spectrum was used to validate a computer simulation model of the 25% relative efficiency Canberra HPGe detector (as used with JET pulse number 92398).

The computer simulation model was used with the Monte Carlo particle transport code MCNP [12] to determine the efficiency of the detector setup with the foils positioned 11 mm above the detector end cap. The evaluated nuclear data library ENDFB.V11 [13] was used in the MCNP calculation.

### 3.4 Development of post-processing toolkit

A post-processing toolkit was developed using Python. This toolkit development was a significant part of this practical foil-spectrometry testing. With this in mind, a number of analysis methods were considered and included as user-defined options when using the toolkit. These methods are described in more detail in this section. The toolkit was developed in a modular approach using functions for improved functionality and future development.

During data acquisition, a dump cycle is established to store pulse by pulse data to an ASCII formatted data file at regular intervals. For each pulse, a time stamp and pulse height are recorded corresponding to the output from the flash analogue to digital convertor in the CAEN hardware. Following data acquisition, a file parser function is called from the Python toolkit, storing the time and pulse data to memory. Using the detector calibration data (shape and efficiency functions) photopeak analysis can be performed on a user defined list of gamma lines.

Nuclide identification from a library of nuclides defined in table 1 is carried out using a spectrum plotting function at user defined time intervals. In addition to user defined time plotting, the spectral plotting function allows the user to manually add colours to highlight photopeaks of interest and produce high resolution plots for reporting (see figure 6 for example).

Using a condensed nuclide library of identified nuclides (see table 2 in the results section), a number of photopeak analysis methods can be carried out. Currently the toolkit allows the user to plot cumulative counts and count rates against time for all nuclides specified in the library, where time binning can be specified manually or in an automated way.

Automated time binning methods include constant bin width, where a user-defined number of equally spaced time bins are used, or equal count bins, where the time bin boundaries are defined so that each bin includes an equal number of events.

Net counts and net count rate are computed by subtracting the Compton continuum in the peak region of interest away from the photopeak. Two algorithms exist within the code to perform this correction; a simplified trapezoidal method and the sensitive non-linear iterative peak (SNIP) algorithm [14]. The trapezoidal algorithm is often well suited to cases where many nuclides are identified, or where many time bins are used as it is less computationally intensive than the SNIP routine. However, for spectra where non-linear features, such as x-rays, Compton edges or backscatter peaks are observed in close proximity to photopeak regions of interest, the SNIP algorithm provides a closer approximation to the true shape of the background. In the trapezoidal algorithm, non-linearities would be averaged, introducing either an under or over estimate to the background depending on the shape of these non-linear features.

Peak widths can also be evaluated in two ways within the toolkit. The full width half maximum (FWHM) can be approximated by the detector shape function for energy E,

$$FWHM(E) = A + B\sqrt{E + CE^2} \quad (2)$$

where A, B and C are parameters determined from a separate calibration measurement. A more sophisticated routine directly evaluates the FWHM of each photopeak by performing a Gaussian fit through all specified regions of interest, using the fitted sigma parameter to evaluate the width.

The toolkit can also calculate the decay corrected count rate at a reference time, the end of the neutron irradiation, ($C_0$). This is calculated by performing an exponential fit to the net count rate against time data determined for each photopeak, using the methods selected from those described above which best suit the data. A time delay parameter ($t_{transfer}$ = 20s for JET pulse number 92398) is used to account for the transfer time between the neutron irradiation environment and the detector.

With knowledge of the detector efficiency (ε) at the photopeak energies analysed, and the relative gamma emission probability (γ) of each gamma line, the end of irradiation activity (also referred to as the initial activity $A_0$) can be calculated using equation 3.

$$A_0 = \frac{C_0}{\varepsilon\gamma} \quad (3)$$

For the results presented in this paper (for JET pulse number 92398) the initial count rate has been determined using the SNIP algorithm and Gaussian shape fitting (as described above). The equal counts time binning method was used with the data fitting 10 times the nuclide half-life (up to the full measurement time).

### 3.5 Neutron spectra unfolding process

MAXED and GRAVEL were used for initial testing and demonstration of the unfolding method to determine the neutron flux spectrum.

As discussed earlier in the paper, as part of the description of a foil-based spectrometer, there are 3 main inputs required to perform an unfolding demonstration. For the data collected from the experiment performed during JET pulse number 92398 the inputs are:

1. The reaction rates, $A_\infty$, as determined from the initial activity ($A_0$) for the photopeaks analysed, can be calculated using equation 4

$$A_\infty = \frac{A_0}{1-\exp(-\lambda t_{pulse})} \quad (4)$$

where $\lambda$ is the decay constant, and $t_{pulse}$ is the pulse length (seconds).

2. The response functions for the materials comprising the Al, Nb and Cr foils (see figure 5).

3. An initial guess spectrum. A selection of different input spectra were tested with the unfolding of this data set.

The response functions are essentially the probability of the nuclear reaction of interest occurring in the foil material and therefore heavily related to the specific reaction cross-section. There are a number of different nuclear data libraries available for the cross-section data and selection of this data can have a significant effect, therefore careful selection of the most appropriate nuclear data libraries is important.

There are also a number of ways to calculate the response function. An approximation to the response function can be determined using the reaction cross-section and material number density,

$$\rho V \int R_m(E)\,dE \quad (5)$$

where $\rho$ is the number density (atoms/barn cm) and $V$ is the volume of the target ($cm^3$) and $R_m(E)$ is the cross-section (barns). However, this approximation does not take into account the effects of neutron flux attenuation, self-shielding, the stack arrangement etc. Therefore, a particle transport calculation (MCNP) was used to calculated the response function of each reaction in individual foils with the correct foil stack geometry and plastic capsule. The response function in $cm^2$ is calculated with MCNP using the equation,

$$\rho V A \int \varnothing(E) R_m(E)\,dE \quad (6)$$

where A is surface area of the foil ($cm^2$), and $\varnothing(E)$ is the energy dependent fluence (particles/$cm^2$).

The response functions in 175 energy bins, calculated using nuclear data from the International Reactor Dosimetry and Fusion File (IRDFF v.1.05) [15] where available and Evaluated Nuclear Data File (ENDF/B-VII.1) [16], are shown in figure 5 for the three reactions used in the unfolding demonstration.

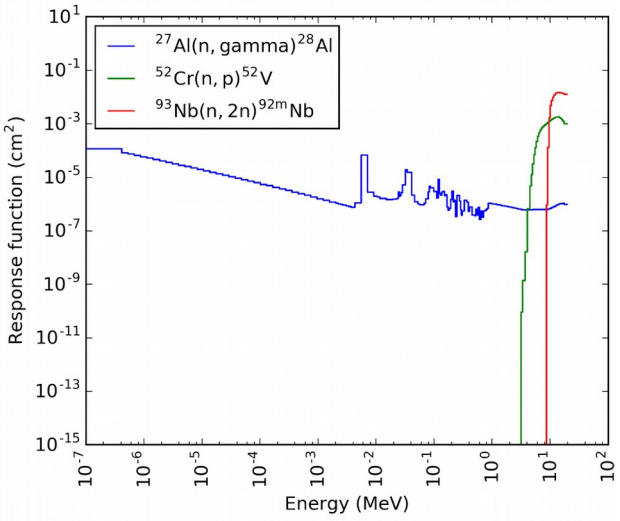


Fig. 5. Foil reaction response functions (in 175 energy bins).

There are ongoing investigations regarding the suitability of using the approximation method to calculate the response functions as this will not require MCNP particle transport calculations to be performed for each energy bin and each experiment. This may be beneficial for quicker analysis of large experimental data sets.

## 4. Results

### 4.1 Experimental results

The experimental data collected from the test in JET pulse number 92398 is presented here. It is foreseen that a foil-based spectrometer system would focus on short-lived radionuclides using a short count time however for this data set a significantly longer measurement time was used. This enabled a large amount of data to be collected from the single pulse test. This large data set was particularly useful for testing the various methods developed in the post-processing toolkit. The gamma spectra measured over the full counting time of 761313 seconds is shown in figure 6. The nuclides identified and used in quantitative analysis of the activity and in turn reaction rates are highlighted. Other photopeaks are observed and are discussed below.

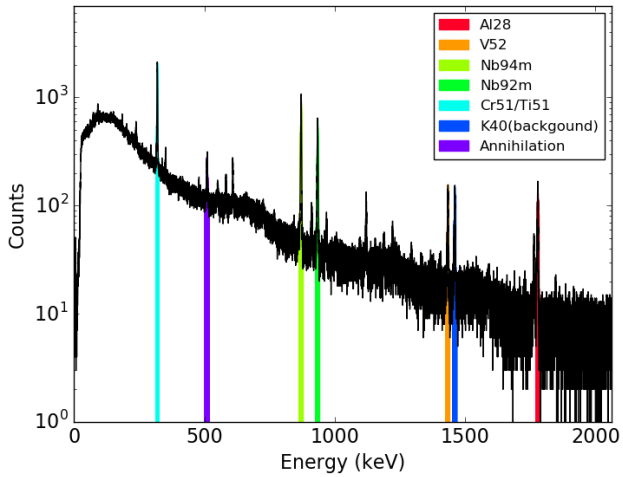


Fig. 6. Gamma spectrometry measurement for JET pulse number 92398 after full measurement time.

### 4.1.1 Gamma spectrometry analysis

The photopeaks in the gamma spectra were initially analysed for the presence of the nuclides listed in table 1. An advantage of the list mode data acquisition is the ability to analyse the gamma spectra over different integral measurement times. This offers advantages in detection limits over conventional acquisition methods. The three nuclides, $^{52}$V, $^{94m}$Nb and $^{28}$Al were identified in the spectra (figure 7) at short measurement times (t < 2000 seconds). The shorter-lived $^{89m}$Y nuclide (half-life of 16 seconds) was not observed.

The Compton continuum, particularly from $^{94m}$Nb, impacts on the detection limit of photopeaks below 871 KeV during measurement times < 2000 seconds. The nuclides of $^{54}$V, $^{27}$Mg and $^{90m}$Y are swamped by the Compton continuum from $^{94m}$Nb and $^{28}$Al. The photopeak of $^{53}$V at 1006 keV is evident but the net counts are too low for accurate quantitative analysis.

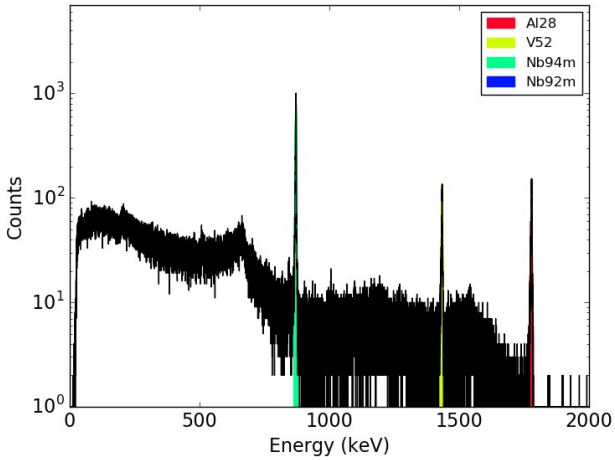


Fig. 7. Gamma spectrometry measurement for JET pulse number 92398 after 2000 seconds.

At longer measurement times (t > 5000 seconds) the longer-lived nuclides, $^{51}$Cr and $^{92m}$Nb were observed more clearly. This is observed in figure 8 where the counts around the 320 keV line are shown for the first 5000 seconds and the next 5000 seconds. The counts of the $^{51}$Ti peak are swamped by the Compton continuum of the $^{94m}$Nb with a similar half-life. By 5000 counts the $^{51}$Ti nuclide will have decayed along with the $^{94m}$Nb and $^{28}$Al which allows the observation of the longer-lived $^{51}$Cr peak.

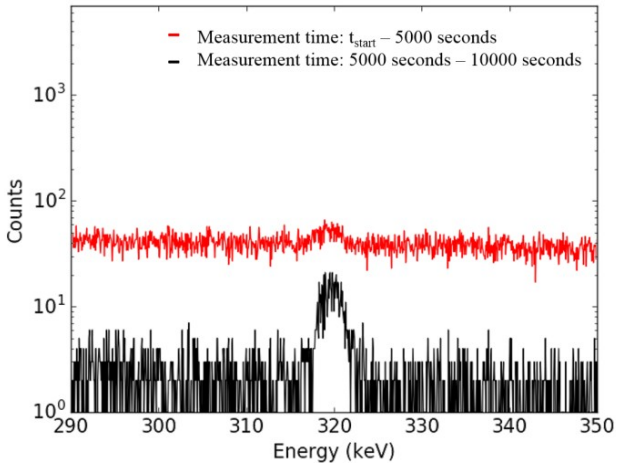


Fig. 8. Counts around 320 keV for first 5000 seconds measurement time and the next 5000 seconds.

### 4.1.2 Determination of foil reaction rates

Using the list mode data acquisition with the developed post-processing toolkit allows for the photopeaks to be analysed at different measurement times. The initial count rate has been determined using the SNIP algorithm and Gaussian shape fitting. The equal counts time binning method was used with the data fitting 10 times the nuclide half-life (up to the full measurement time).

The reaction rates in table 2 were derived from the initial count rate using equations 3 and 4. The uncertainty values quoted in table 2 are propagated from the Poisson statistical error associated with each photopeak, and also the errors on the fit parameters determined in the decay correction process.

Table 2. Reaction rates determined from photopeak analysis. The results in italics are currently not used in the final unfolding calculation due to ongoing investigations regarding the reaction response function.

| Measured nuclide | Initial activity (Bq) | Uncertainty (%) | Reaction rate (reactions/s) |
|---|---|---|---|
| $^{28}$Al | 6.22E+03 | 7.4 | 1.13E+05 |
| $^{52}$V5 | 2.18E+03 | 5.9 | 6.55E+04 |
| *$^{94m}$Nb* | *1.21E+06* | *3.9* | *6.01E+07* |
| $^{92m}$Nb | 3.98E+00 | 2.2 | 4.58E+05 |

### 4.2 Demonstration of neutron spectrum unfolding

The spectrum in the KN2 3U location has previously been determined through an MCNP calculation using a

computational model of the JET facility [17]. This MCNP calculated spectrum was used as the 'a priori' best guess spectrum input for the neutron unfolding demonstration.

By folding this flux spectrum with the reaction response functions, we can compare the calculated reaction rates with those measured (see table 3). The calculated reaction rates agree with the measurements within 2% – 18%, further validating this 'best guess' calculated spectrum.

Table 3. Comparison of measured and calculated reaction rates.

| Reaction | Reaction rate (reactions/s) | | C/E |
|---|---|---|---|
| | Calculated | Measured | |
| $^{27}Al(n,\gamma)^{28}Al$ | 1.34E+05 | 1.13E+05 | 1.18 |
| $^{52}Cr(n,p)^{52}V$ | 5.80E+04 | 6.55E+04 | 0.89 |
| $^{93}Nb(n,2n)^{92m}Nb$ | 4.47E+05 | 4.58E+05 | 0.98 |

Using this data with the unfolding codes of MAXED and GRAVEL produces output spectra presented in figure 9. The difference in total flux for the GRAVEL and MAXED unfolded spectrum was -15% and +2% respectively.

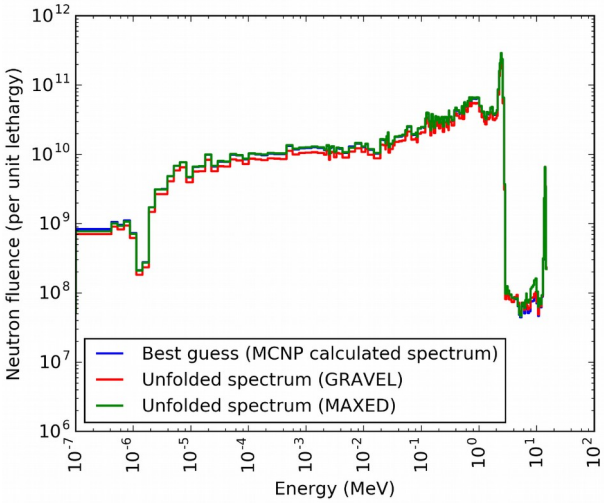


Fig. 9. Comparison of unfolded spectra and MCNP calculated spectrum, using MCNP calculated spectrum as best guess input.

As only three reaction rates were used in this unfolding demonstration, include the two threshold reactions of $^{52}Cr(n,p)^{52}V$ and $^{93}Nb(n,2n)^{92m}Nb$, and the $^{27}Al(n,\gamma)^{28}Al$ reaction, the unfolding codes had limited data for unfolding 175 energy bins. Variations in the flux spectra are mostly limited to the energy bins above 5 MeV, where the 2 threshold reactions are present (see figure 10). The difference in the unfolded spectra and the calculated MCNP spectrum is shown in figure 11, as the unfolded divided by the calculated.

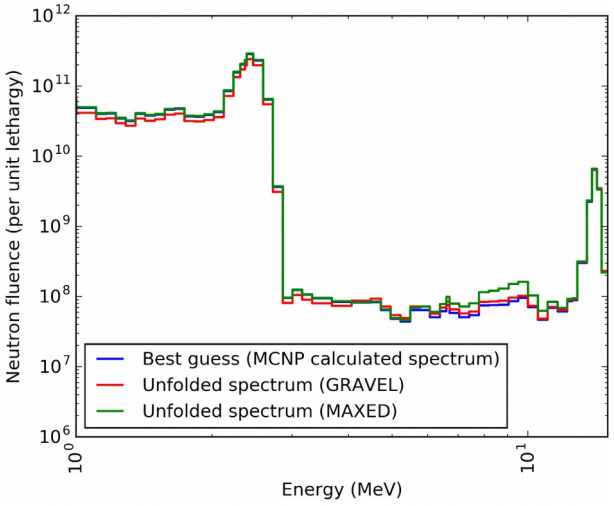


Fig. 10. Comparison of spectra as in figure 9 > 1MeV.

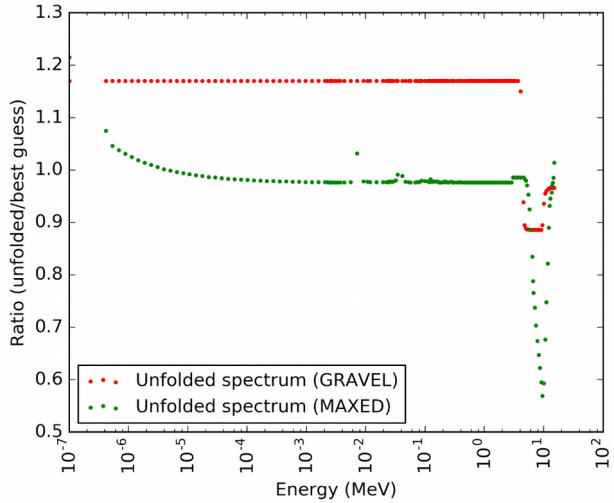


Fig. 11. Difference in the unfolded (GRAVEL and MAXED) spectra with the MCNP calculated spectrum.

By using a modified input spectrum, through reducing the flux by 2 orders of magnitude, the use of the unfolding codes can be more readily observed. We can see how the unfolding codes have used the provided three reaction rates to re-normalise the flux spectra (figure 12).

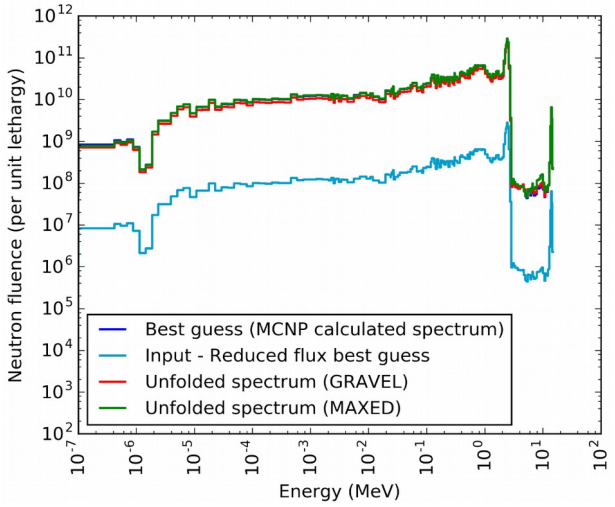

Fig. 12. Comparison of unfolded spectra and MCNP calculated spectrum, using reduced flux MCNP calculated spectrum as guess input.

## 5. Conclusions

The proposed method for testing of the TBMD foil spectrometer, and associated hardware, during a JET D-T campaign has undergone functional and development testing during the D-D campaign (reference C36b). The method will be used to determine the tritium production rates in ITER TBMs to validate the nuclear design of tritium breeder blanket concepts. The JET D-D test has provided important testing of post-processing techniques for analysis of large data sets, through the use of list mode data collection, and of the detector set up and measurement system.

The post-processing toolkit developed for analysis of the large list mode data set enables spectra to be plot at various times and peak analysis using various background correction methods, time binning and measurement time.

An advantage of the list mode data acquisition was illustrated in the analysis of lower activity longer-lived nuclides such as $^{51}$Cr (half-life = 27 days). This nuclide would likely not be observed in conventional gamma spectroscopy measurements as the contribution of shorter-lived high activity nuclides to the Compton continuum would inhibit the detection of the $^{51}$Cr photopeak. Analysing the gamma spectrum over a time period commencing 5000 seconds after irradiation enables the $^{51}$Cr photopeak to be more clearly observed

To demonstrate the system, post-processing and unfolding, some key peaks were identified for quantitative assessment. Significantly this included some of the threshold reactions resulting from the D-T neutrons that are present during D-D plasma.

Some of the photopeaks of interest, particularly those below 871 keV, were not observed due to the Compton background of the $^{94m}$Nb and $^{28}$Al nuclides. It is proposed that in future testing further pre-analysis is performed to determine a more optimum foil stack order and thickness of foil. In this experiment (in JET pulse number 92398) the short measurement time gamma spectrum is dominated by the $^{94m}$Nb and $^{28}$Al. Preliminary analysis of other earlier experiments had led to the decision to reduce the thickness of the Al foil to 0.1 mm and to place at the back. A reduction in the amount of Nb, with an increase in the thickness of Cr should assist in reducing the impact of the $^{94m}$Nb Compton background on detection limits, and could be tested in future D-D JET operations.

The gamma spectrum, neutron flux spectrum and reaction rates will be different in D-T conditions and in a TBM position, however this testing utilising the D-D fusion conditions in JET has provided a unique opportunity to demonstrate the use of a foil-based spectrometry system and develop a post-processing toolkit.

## 6. Future work

There is ongoing work to analyse further data collected as part of the WPJET3 TBMD subproject from the other JET pulses using a similar setup, and to extrapolate to very high efficiency detectors such as the 190% relative efficiency detector.

Further development of the python toolkit will also take place, including investigations into methods for handling coincident summing corrections and gamma spectrometry predictions experiment planning.

The methods for unfolding are being further investigated including the potential for use of a new genetic algorithm process and with more complex spectra e.g. T-T.

## Acknowledgments

This work has been carried out within the framework of the EUROfusion Consortium and has received funding from the Euratom research and training programme 2014-2018 under grant agreement No 633053 and from the RCUK Energy Programme [grant number EP/I501045]. The views and opinions expressed herein do not necessarily reflect those of the European Commission.

## References

[1] P. Batistoni, D. Campling, S. Conroy, et al., "Technological exploitation of Deuterium-Tritium operations at JET in support of ITER design, operation and safety," *Fusion Eng. Des.*, vol. 111, no. 2016, pp. 278–285, 2015.

[2] A. Klix, A. Domula, U. Fischer, et al., "Test facility for a neutron flux spectrometer system based on the foil activation technique for neutronics experiments with the ITER TBM," *Fusion Eng. Des.*, vol. 86, no. 9–11, pp. 2322–

2325, 2011.
[3] D. Leichtle, M. Angelone, P. Batistoni, et al., "The F4E programme on nuclear data validation and nuclear instrumentation techniques for TBM in ITER," *Fusion Eng. Des.*, vol. 89, no. 9–10, pp. 2169–2173, 2014.
[4] M. Angelone, U. Fischer, D. Flammini, et al., "Neutronics experiments, radiation detectors and nuclear techniques development in the EU in support of the TBM design for ITER," *Fusion Eng. Des.*, vol. 96–97, pp. 2–7, 2015.
[5] A. Klix, A. Domula, U. Fischer, et al., "Neutronics diagnostics for European ITER TBMs: Activation foil spectrometer for short measurement cycles," *Fusion Eng. Des.*, vol. 87, no. 7–8, pp. 1301–1306, 2012.
[6] M. Reginatto, "The 'Few-Channel' Unfolding Programs in the UMG Package: MXD_FC33, GRV_FC33 and IQU_FC333," *Phys. Bundesanstalt*, 2004.
[7] W. N. McElroy, S. Berg, T. Crockett, et al., "A computer-automated iterative method for neutron flux spectra determination by foil activation. Volume 1. A study of the iterative method." 1967.
[8] L. R. Greenwood & C. D. Johnson, "User Guide for the STAYSL PNNL Suite of Software Tools," *Pnnl-22253*, no. February, 2013.
[9] Goodfellow, "Goodfellow Catalogue." [Online]. Available: http://www.goodfellow.com/catalogue. [Accessed: 01-Sep-2016].
[10] B. Pritychenko, E. Běták, M. A. Kellett, et al., "The Nuclear Science References (NSR) database and Web Retrieval System," *Nucl. Instruments Methods Phys. Res. Sect. A Accel. Spectrometers, Detect. Assoc. Equip.*, vol. 640, no. 1, pp. 213–218, Jun. 2011.
[11] CAEN, "User Manual UM3246 DT5724," 2017.
[12] D. Pelowitz et al., "MCNP6 Users Manual – Code Version 1.0, LA-CP-13-00634 Rev 0."
[13] M. B. Chadwick, P. Obložinský, M. Herman, et al., "ENDF/B-VII.0: Next Generation Evaluated Nuclear Data Library for Nuclear Science and Technology," *Nucl. Data Sheets*, vol. 107, no. 12, pp. 2931–3060, Dec. 2006.
[14] M. Caccia, A. Ebolese, M. Maspero, et al., "Background removal procedure based on the SNIP algorithm for γ − ray spectroscopy with the CAEN Educational Kit," pp. 1–4.
[15] R. Capote, K. I. Zolotarev, V. G. Pronyaev, et al., "International Reactor Dosimetry and Fusion File IRDFF," *J. ASTM Int.*, vol. 9, no. 4, 2012.
[16] M.B. Chadwick et al., "ENDF/B-VII.1: Nuclear Data for Science and Technology: Cross Sections, Covariances, Fission Product Yields and Decay Data," *Nucl. Data Sheets 112(2011)2887*.
[17] P. Batistoni, S. Conroy, S. Lilley, et al., "Benchmark experiments on neutron streaming through JET Torus Hall penetrations," *Nucl. Fusion*, vol. 55, no. 5, p. 53028, 2015.